Building-Integrated Agriculture (BIA) In Urban Contexts: Testing A Simulation-Based Decision Support Workflow

Khadija Benis[1], Christoph Reinhart[2], Paulo Ferrão[1]

[1] IN+ Center for Innovation, Technology and Policy Research, IST, Lisbon, Portugal
[2] Building Technology, Massachusetts Institute of Technology, Cambridge, USA

Corresponding author e-mail: khadija.benis@tecnico.ulisboa.pt

Abstract

Building-Integrated Agriculture (BIA) in urban areas is claimed to be environmentally sustainable vis-à-vis conventional commercial agriculture practices by reducing food miles, minimizing land and water use and improving yields. However, as it is operated in controlled indoor environments, BIA can be highly energy-intensive. In order to better understand the influence of local foodshed characteristics, climate conditions and farm properties on the environmental performance of BIA systems, this article applies a performance-based parametric simulation workflow for BIA that incorporates daylight, energy, crop growth and water models, to (a) Rooftop Greenhouse (RG) farms and (b) Shipping Container (SC) farms located in the cities of Lisbon, Singapore, Paris and New York. Results show that – while RG farms can significantly reduce GHG emissions under all the tested climates – SC farms may only have a positive overall environmental impact in megacities located in colder climates, that seasonally rely on long distance food imports.

Introduction

Historically, the growth of cities was closely linked with the development of agriculture in their hinterlands, where surpluses of food led to the establishment of settlements that sprawled and became cities. Over the last century, this dependency has progressively disappeared, giving way to global food production and distribution systems and their inherent urban-rural dichotomy (Steel, 2008). Today, feeding the world's sprawling cities is increasingly recognized to be a major challenge since food systems are part of complex global networks of cultivation, processing, storage and distribution, highly vulnerable to any geopolitical, economic, or natural disaster-related crises. On an environmental level, food consumed in urban areas is usually not only transported over longer distances, raising concerns about "Food Miles" greenhouse gas (GHG) emissions (Weber and Matthews, 2008), but an estimated one-third of global food production is lost or wasted in the process (FAO, 2011).

While it is neither possible nor environmentally desirable to stop global urbanization, bringing food production back within the limits of cities is feasible through Urban and Periurban Agriculture (UPA), which can potentially contribute to mitigate environmental impacts of urban food systems (Benis and Ferrao, 2016). While cattle raising or production of cereals, oilseeds and pulses require large periurban areas of land, horticultural crops offer high yields in small areas and can thus be easily grown in urban gardens, backyards, vacant lots, rooftops or even indoors. Among existing methods for growing vegetables in the city, Building-Integrated Agriculture (BIA), which consists of the application of high-performance soilless cultivation methods adapted for use on top of or in buildings (Puri and Caplow, 2009), is claimed to be environmentally sustainable by reducing food miles (Specht et al., 2014), minimizing land use and water consumption (Sanye-Mengual et al., 2015) and improving yields (Despommier, 2013).

Rooftop Greenhouse (RG) farming is an expanding form of BIA in developed countries where urban land is expensive, rooftops represent a considerable unutilized area, and Controlled-Environment Agriculture (CEA) technologies allow for year-round cultivation of any horticultural crop independently of local climatic conditions. Another emerging trend in the field of CEA are Shipping Container (SC) farms. Equipped with state-of-the-art climate control technology and hydroponic growing equipment, SC farms allow for year-round production and can be installed in vacant lots, warehouses, basements or rooftops. However, CEA can be highly energy-intensive. Depending on local climatic conditions and specific crop requirements, producing food locally in artificially controlled environments has been shown to sometimes have greater environmental impacts than importing produce from elsewhere (Kulak et al., 2013). The net impact depends on emissions caused by energy use for greenhouse operation versus avoided transportation-related emissions. These trade-offs should therefore be carefully measured.

Several researchers have shown the great potential of improving energy efficiency of agricultural production facilities that lies in the use of Building Performance Simulation (BPS) tools. Over the past few years, climate-based simulations with integrated plant growth models were built within ESP-r, TRNSYS and EnergyPlus, to evaluate thermal behavior of agricultural greenhouses (Carlini and Castellucci, 2010; Marucci et al., 2013; Alvarez- Sánchez et al., 2014), and assess passive design strategies such as natural ventilation (Mashonjowa et al., 2013), adaptive shells (Lee et al., 2013) or potential heat exchanges between a rooftop greenhouse and its host building (Ward et al., 2015). This expanding literature validates the use of BPS tools for performance simulation of agricultural production facilities. Furthermore, BPS programs allow for connectivity with algorithm editors such as MATLAB/Simulink –which was used to predict irrigation water consumption through mathematical evapotranspiration models (Pamungkas et al., 2014). In contrast, simulation programs such as KASPRO (De Zwart, 1996) that have been custom-developed for agricultural greenhouses, do not offer this flexibility and cannot model HVAC components or airflow with the same rigor as BPS programs (Lee et al., 2012).

While previous BIA studies using BPS tools considered lighting, climate control, passive systems and water consumption separately, the authors are not aware of a tool that combines all of these parameters into an integrated workflow that allows the user to evaluate a BIA project in a holistic way. Integrating these sub-models is crucial, as they often influence each other: e.g., while supplemental artificial lighting provides the plants with optimal growing conditions, contribution of heat from lighting systems to the overall heating requirements of a farm can be significant (Dorais, 2003). Furthermore, unlike conventional rural ground-based greenhouses, BIA urban farms have to be designed according to urban context-related constraints such as a limited rooftop area, the orientation of the host building, or shadings from surrounding buildings. To fill this gap, the authors recently developed a fully integrated simulation workflow that gives decision-makers in urban context actionable feedback for design decision-making related to implementing BIA in a given neighborhood (Benis et al., 2017).

In this manuscript, this method is systematically applied for a variety of cities world-wide in order to better understand the overall potential for BIA to reduce food-related carbon emissions in these locations. If the overall assessment of a region is favorable, the workflow, which is based on climate data, crop requirements and farm geometry, can be further used by architects and urban planners to assess the viability of BIA for a specific site.

Materials and methods

This section presents a description of the BIA performance-based simulation workflow, which was developed using the architectural 3D modeling program Rhinoceros 5.0™ (McNeel, 2016) along with its graphical algorithm editor plug-in Grasshopper™. The latter enables the use of numerous environmental analysis plug-ins such as DIVA-for-Rhino (Jakubiec and Reinhart, 2011) that are based on the validated daylighting and thermal simulation engines DAYSIM and EnergyPlus.

The aim of the workflow is to help the user to design a local BIA system and optimize crop yields and energy consumption. The workflow consists of the following five steps: (1) Site description; (2) Farm builder; (3) Operation model; (4) Plant growth and water models; (5) Results visualization and model adjustments (see **Figure 1**). Simulation outputs include food production, water use and energy use.

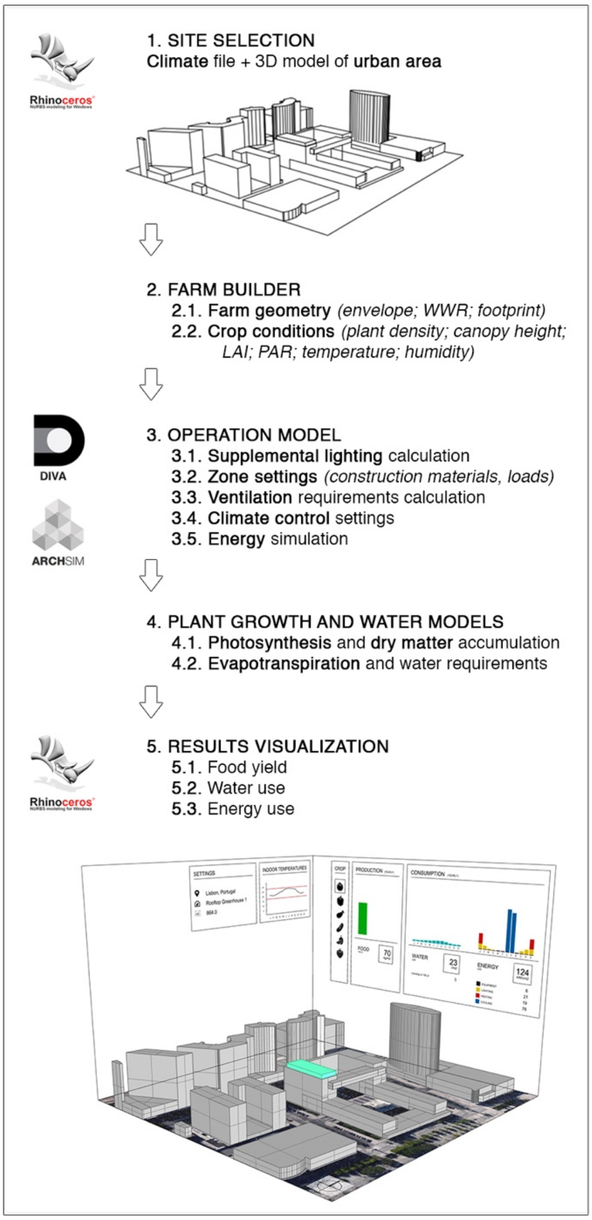

Figure 1: Simulation workflow for BIA.

Step 1: Site description

During *site description*, an EnergyPlus weather file (EPW format) containing the annual climate data of the project location is imported from the EnergyPlus weather database (EnergyPlus, 2016), and the 3D model of the urban area in focus is either imported from GIS or LiDAR or manually generated within CAD.

Step 2: Farm builder

The *farm builder* step consists of selecting the geometry of the farm and the crop species to be grown as inputs for steps 3 and 4. The outer boundary of the farm is abstracted as a simple box located within a specific urban location, i.e., on a rooftop or at any chosen building floor. The *farm builder* decomposes the box into components of the farm, i.e., its footprint and envelope, to which it affects window-to-wall ratios (WWR) that can be altered. According to the type of farm that was selected, structural specificities and construction materials are assigned to the model for the thermal simulation in step 3. For greenhouses, structure and covering materials can be chosen from a selection of typical materials which are widely used in greenhouses. For indoor farms, envelope materials are set according to the host building. Material properties such as thermal conductivity and light transmissivity are embedded in the material selection.

Step 3: Operation model

Operational energy for equipment, supplemental lighting and space heating and cooling account for a substantial share of the environmental impact of a BIA farm. The operation model simulates these loads.

Supplemental lighting schedule

Plants have a similar action spectrum as the human eye, which is why the RADIANCE-based annual daylighting simulation program DAYSIM is used in this model through the DIVA-for-Rhino Grasshopper plug-in (Reinhart and Walkenhorst, 2001).

In controlled environments, Photosynthetically Active Radiation (PAR) from available daylight is usually complemented with PAR from supplemental artificial light, in order to reach the PAR that is required by the crop to achieve optimal growth throughout the year. To calculate PAR from daylight, a grid of upward facing illuminance sensors with a resolution of 1m x 1m is placed within the farm box at the top of the plant canopy. The simulation generates daylight illuminance values (in lux) for each sensor point, for each hour of the year. Based on the difference between the optimal PAR of the selected crop species and these hourly results, the deficit of PAR will represent the needs of supplemental artificial lighting that then serves as an input of the thermal model in the form of an annual lighting schedule.

Thermal model

Within our workflow, we are using the US Department of Energy's EnergyPlus whole building thermal simulation engine to model operational energy use in the urban farms (U.S. Department of Energy, 2016). The simulations are set up and run through the Archsim Grasshopper™ component which forms part of the DIVA-for-Rhino v4 suite. For that purpose, the urban farm geometry from Step 2 serves as an input to the thermal model. Total yearly energy use is expressed in kWh/m^2/y, and this value is disaggregated into four categories: (1) equipment; (2) lighting; (3) heating; and (4) cooling.

Step 4: Plant growth and water models

Plant growth model

Existing research on horticultural crop growth (De Zwart, 1996; Vanthoor, 2011) was used here as a basis of our model. Light quantity (intensity over time) and quality (spectral distribution), i.e., PAR, temperature and air-CO_2 concentration have decisive impact on the net photosynthesis rate and therefore on crop growth (Vanthoor, 2011). These three variables are used as inputs of the plant growth model. Built upon earlier crop yield models that simulate carbohydrate distribution to plant organs, Vanthoor's model is more accurate as it integrates the effect of temperature variations on photosynthesis rate. The model was validated for large temperature ranges. Given its complexity, it is not described in this paper.

Evapotranspiration model

Crop water requirement corresponds to the volume of water that a plant needs to maintain maximum rates of evapotranspiration (ET). Stanghellini's climate and crop-based model, which was established to be the more reliable for predicting ET in controlled-environment high-tech greenhouses (Villarreal-Guerrero et al., 2012; Pamungkas et al., 2014), was built here within Grasshopper.

Step 5: Results visualization and adjustments

The workflow was implemented in a Grasshopper™ script that includes a simple dashboard view of the simulation results for three categories: (1) yearly food yield per square meter; (2) monthly water use per square meter; and (3) monthly energy use per square meter. The simulations can be iteratively run to optimize results according to specific project-related performance criteria.

Case studies and simulation inputs

Potential for mitigating environmental impacts of food production depends on specific conditions of a given urban food system, i.e., on the level of technology and efficiency of the existing cultivation facilities, and on the transportation mode and distance traveled by the crop to reach the city (Benis and Ferrao, 2016). The above described BIA simulation workflow was applied to hypothetical urban farms with hydroponic tomato production and assessed against conventional tomato supply chains of four metropolitan areas – Lisbon, Singapore, Paris and New York – to shed light on the extent to which higher yields and lower transportation distances can offset operational and transportation-related energy use intensity of BIA across climate conditions and metropolitan scales.

Tomato was selected here as a crop due to the vast existing literature about controlled-environment soilless production of tomato and to the availability of data on fresh tomato supply chains for the four investigated metropolitan areas.

Baseline models

Baseline models represent the current situation in the four metropolitan areas, including (1) per capita demand for fresh tomato (kg/cap/y); (2) origin of supply (i.e., local vs. imported produce) and average distance traveled; (3) average yield under current cultivation methods (kg/m^2); (4) water use intensity (l/kg); and (5) operational and transportation-related energy use intensity of produce (kWh/kg).

Table 1 summarizes the assumptions of the baseline models.

Table 1: Assumptions of the baseline models.

Metropolitan area	**Lisbon**	**Singapore**	**Paris**	**New York**
Population (10^6 inhabitants)	2.8	5.5	12.4	23.7
Demand for fresh tomato (kg/cap/y) **Local supply** (%) **Imported supply** (%)	10.4 14 86	6.7 0 100	13.9 0 100	9.5 9 91
Origin of supply	Portugal (60%); Spain (30%); Morocco (10%)	Malaysia (93%); Viet Nam (2%); Thailand (1%); Netherlands (1%); Indonesia (1%); China (1%); Australia (1%)	France (40%); Morocco (41%); Spain (19%)	USA (55%); Mexico (38%); Canada (7%)
Average yield (kg/m^2) **Farm typology**	16.5 Greenhouse (unconditioned, ground-based)	10.0 Open-field and low-tech greenhouse	29.7 High-tech greenhouse (40%); greenhouse (unconditioned) (60%)	13.0 Open-field (93%); High-tech greenhouse (7%)
Water use (l/kg) $\mathbf{GWP_{Irrigation}}$ ($kgCO_2eq/kg$)	40.0 0.706	30.0 0.900	35.5 1.766	42.0 0.360
Energy (growing process) (kWh/kg) $\mathbf{GWP_{Energy}}$ ($kgCO_2eq/kg$)	0.130 0.049	0.870 0.638	2.714 1.036	0.561 0.245
Distance traveled (tkm) $\mathbf{GWP_{Freight}}$ ($kgCO_2eq/kg$)	0.556 0.278	0.672 0.336	1.865 0.933	3.260 3.252
Total GWP ($kgCO_2eq/kg$)	1.033	1.874	3.734	3.857

Average yields and "food miles"

Based on respective shares of origins of tomato supply and on the farming techniques that are practiced in these different locations, average yields of existing tomato supply chains were calculated:

$$YIELD_{AV} = \sum_{i=1}^{n} w_i YIELD_i \quad (1)$$

where $YIELD_{AV}$ is the weighted average yield of the tomato currently supplied to the city (kg/m^2); w_i is the relative weight of each origin of supply; and $YIELD_i$ are the respective tomato yields for each location (kg/m^2), which vary according to local climatic and technological conditions, and were found in the literature (Albright and Villiers, 2008; FAOSTAT, 2013; Payen et al., 2015; Sanye-Mengual et al., 2015).

According to the UN classification, Lisbon and Singapore are medium-sized cities, i.e., cities of 1 to 5 million inhabitants. One in five urban dwellers currently lives in a medium-sized city. While labeled as "medium-sized", these agglomerations are in fact the biggest cities in 79 countries or areas, such as Oceania and many European countries (United Nations, 2014). Lisbon's metropolitan area relies heavily on imports to meet the demand for vegetables of its inhabitants: currently, only 14% of the fresh tomato that is consumed in the agglomeration is produced within the region, while the rest is supplied by other parts of the country as well as by Spain and Morocco. On average, an imported tomato travels a distance of 556 km to reach the city (Benis and Ferrao, 2016). The wealthy island of Singapore, with over 5 million residents, is one of the most densely populated cities in the world. Since agricultural land is scarce, the island relies heavily on overseas imports of horticultural crops. Fresh tomatoes are shipped from neighboring countries such as Malaysia (93%), Viet Nam, Thailand, Indonesia and China, traveling an average distance of 672 km to reach Singapore. Paris and New York belong to the category of megacities, i.e., cities with a population of more than 10 million inhabitants. Fresh tomato travels an average distance of 1,865 km to reach the Paris metropolitan area. Around 40% stem from other parts of France while the rest is imported from Morocco and Spain (FAOSTAT, 2013; Payen et al., 2015). In New York, 9% of the fresh tomato are grown in-state. The rest comes from other states (mainly California and Florida) as well as Mexico and Canada, traveling an average distance of 3,260 km before reaching the New York metropolitan area (Albright and Villiers, 2008).

Global Warming Potential (GWP)

Additionally, GHG emissions related to irrigation, operational energy and transportation of existing supply of fresh tomato to the four metropolitan areas were calculated ($kgCO_2eq/kg$), using the relevant emission factors:

$$GWP = \sum_{i=1}^{n} w_i \left(WU_i \times E_i^{IR} + EU_i \times E_i^{EL} + F_i \times E_i^{TR}\right) \quad (2)$$

where GWP is the Global Warming Potential of the tomato currently supplied to the city ($kgCO_2eq/kg$); w_i is the relative weight of each origin of supply; WU_i is the water use per kilogram of tomato, (l/kg); EU_i is the energy use per kilogram of tomato (kWh/kg); F_i represents the freight transport of one ton of tomatoes over a distance of one kilometer (tkm); and E_i^{IR}, E_i^{EL} and E_i^{TR} are the respective emission factors of irrigation, electricity generation and refrigerated truck transportation for each origin of supply.

Alternative BIA scenarios

In the alternative urban farming models that were tested here, all the fresh tomatoes consumed in the four metropolitan areas were assumed to be produced within the borders of the agglomerations, in (a) RG farms and (b) SC farms, and to travel an average distance of only 30 km before reaching distribution points.

For the simulation, technology and construction properties of sample farms were defined according to the most widespread properties of existing facilities (see **Figure 2**). Common features of high-tech RG farms include structures made of steel, polycarbonate covers, NFT hydroponic equipment, backup lighting and HVAC systems. On the other hand, SC farms are opaque boxes with no penetration of daylight, built inside insulated shipping containers outfitted with hydroponic equipment, climate control technology and lighting systems.

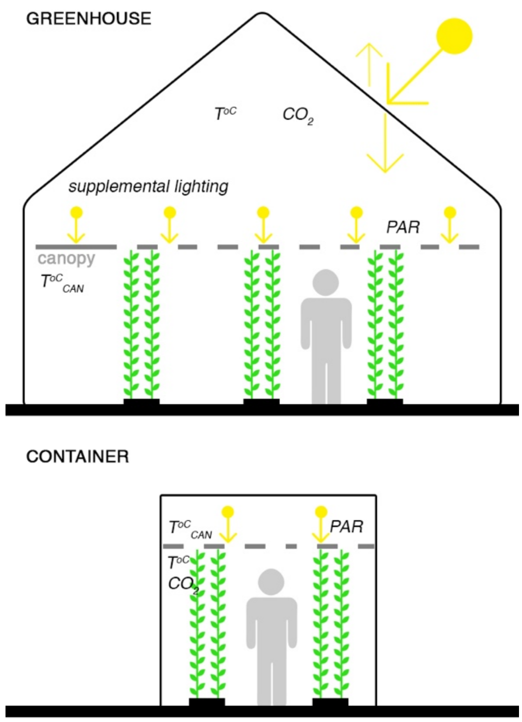

Figure 2: Sections of BIA farms.

Table 2 shows the simulation inputs. Climate control was set in order to maintain indoor temperatures within the optimal range for tomato growth, i.e., between 17 and 28°C (Kittas et al., 2013). A Ground Source Heat Pump was considered for providing HVAC to the urban farms. The Coefficient of Performance (COP) of heating was assumed to be 3.1 and the COP of cooling was assumed to be 3.93 (ASHRAE, 2015). For supplemental lighting, High-Pressure Sodium (HPS) lamps have traditionally been the most efficient lighting source in converting electric energy into useful light for photosynthesis (Dorais, 2003). These lamps are widely used in commercial hydroponic facilities and were therefore considered here. Finally, it was assumed that the rooftop greenhouses were not receiving any shading from the surrounding buildings and that the shipping container farms were also located on unshaded rooftops.

Table 2: Simulation inputs of the sample urban farms.

	RG Farm	SC Farm
GEOMETRY		
Altitude (m)	30	
Orientation	N-S	
Footprint (m^2)	1,000	28*
Height (m)	5	2.5
WWR (%) (all faces)	85	0
MATERIALS		
Structure	Steel	Aluminium
Cover	Polycarbonate	-
Shading	Polyester	-
Insulation	-	PUR (70mm)
SUPPLEMENTAL LIGHTING		
Lighting system	HPS lamps	
CLIMATE CONTROL		
Heating COP	3.1	
Cooling COP	3.93	
Mean CO_2 ($\mu mol.mol^{-1}$)	400	
Humidity (%)	60-90	
CLIMATE		
Lisbon (38°N,9°W)	Csa (Tropical Mediterranean)	
Singapore (1°N,103°E)	Af (Tropical Rainforest)	
Paris (48°N,2°E)	Cfb (Oceanic)	
New York (40°N,74°W)	Cfa (Humid Subtropical)	
CROP (TOMATO)		
Canopy height (m)	2	
Plant density (plants/m^2)	4	
Photoperiod (h)	13	
LAI	2.6	
PAR_{opt} (mol/m^2/day)	20	

* Dimensions of a standard 12m container type were considered here.

Results and discussion

Food production and water use

Optimal growing conditions of NFT hydroponic tomato were assumed to be achieved year-round in the conditioned urban farms, with an available PAR of 20 mol/m^2/day and temperatures ranging from 17 to 28°C (the plant growth model uses hourly temperature data from the thermal model as an input). Under these conditions, simulations showed that yearly yields of 67 to 76 kg/m^2 can be achieved. These yield variations are due to temperature fluctuations in the farms along the year (see indoor temperature charts in **Figure 6**) —as mentioned previously, temperature fluctuations have a direct impact on photosynthesis and therefore on dry matter accumulation (Vanthoor, 2011).

When compared to current supply chains for tomato in the four case studies, BIA farms can lead to efficiency gains of a factor of 2.4 (in Paris) up to 6.9 (in Singapore) (see **Figure 3**). This high productivity is both due to the year-round production that is allowed by CEA, and to the higher plant density that is supported by soilless culture systems. The goal of controlled-environment agriculture is to prolong conventional open-field growing periods towards year-round food production and therefore increase profitability. Here, simulation results show yearly tomato yields that vary around 70kg/m^2, which is aligned with existing practice in high-tech conditioned farms (Goldstein et al., 2016). These simulated yields can be further optimised, by setting temperatures and CO_2 concentrations within a more optimal range.

On the other hand, simulated BIA farms use 3 to 6 times less water than conventional systems (see **Figure 4**). This result is aligned with existing literature establishing that hydroponic systems utilize water in a more efficient way than conventional on-soil farming (Barbosa et al., 2015; Sanye-Mengual et al., 2015). While the volume of water consumed by the plant is identical in both systems, hydroponic systems deliver the water more efficiently, with a larger percentage of water going to plant evapotranspiration, whereas in conventional on-soil systems, water that is not rapidly absorbed by the roots is lost to percolation. Similarly, efficiency gains of a factor of 6.6 were found in an analogous comparative study (Barbosa et al., 2015).

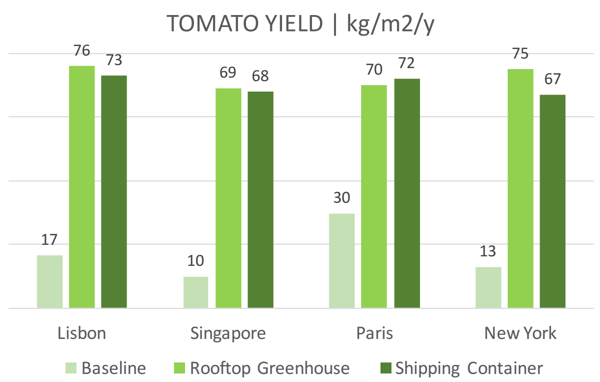

Figure 3: Yearly tomato yield of existing supply systems vs. simulated urban farms.

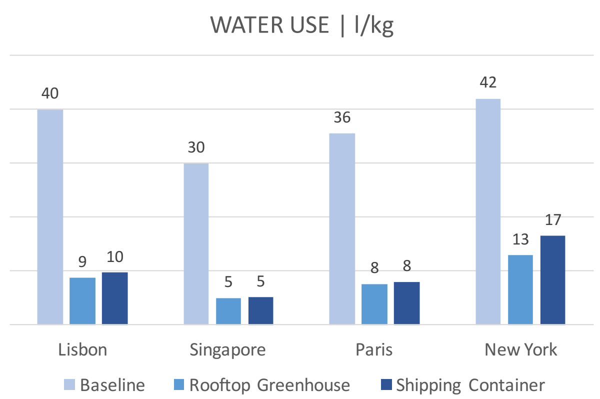

Figure 4: Water use in existing supply systems vs. simulated urban farms.

Operational energy use

Indoor crop production demands significant climate control measures to artificially provide plants with optimal growing conditions. Here, climate control was set in order to maintain temperatures within the optimal range for tomato growth, i.e., 17 to 28°C. Under all the simulated scenarios, operational energy use is higher in BIA farms than in existing supply systems (see ***Figure 5***).

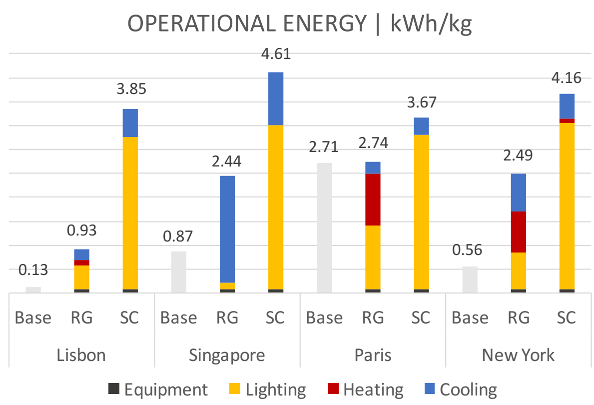

Figure 5: Operational energy consumption of existing supply systems vs. simulated urban farms.

Baseline

In Lisbon, the significantly low energy intensity of tomato under the current supply chain (0.13 kWh/kg) can be explained by the fact that it is essentially produced in unconditioned low-tech greenhouses in Portugal, Spain and Morocco, under mild Mediterranean climate conditions that provide a good growing environment for horticultural crops with medium thermal requirements such as tomato (Benis et al., 2017). Similarly, tomato is imported to Singapore from neighbouring countries where it is essentially grown in low-tech greenhouses (0.87 kWh/kg), and to New York from open-field and low-tech greenhouse cultivation in California, Florida and Mexico (0.56 kWh/kg) (Albright and Villiers, 2008). On the other hand, the substantially higher energy intensity of the base model for Paris (2.71 kWh/kg) is due to the fact that 40% of the tomato comes from conditioned high-tech French greenhouses (Payen et al., 2015) (see **Table 1**).

Simulated scenarios

In the simulated RG farms, heating and cooling requirements represent the largest share of operational energy consumption. These loads can be reduced by testing alternative greenhouse shells with enhanced thermal properties. Moreover, temperatures were kept here within the optimal range for tomato, as described in the literature (Kittas et al., 2013). Energy savings can be achieved by further optimising this range. Whereas changing heating and cooling set points can admittedly lead to higher energy loads for climate control, these variations can be balanced by improving the greenhouse shell and by reducing lighting loads.

Figure 6: Energy loads (kWh/m^2/y) and average indoor temperatures (°C) in the simulated urban farms.

On the other hand, SC farms do not receive any natural light and therefore supplemental lighting constitutes the largest share of energy consumption. A power intensity of 47 W/m^2 is necessary through photoperiods of 13 hours during the whole year, resulting in an energy consumption of 232 kWh/m^2/y for supplemental lighting. More efficient artificial light sources like LED can be assessed against HPS lamps to decrease energy consumption related to supplemental lighting.

Furthermore, depending on light levels, the contribution of heat from the lighting system to the overall heating and/or cooling requirements of the farm can vary significantly. In a greenhouse in Quebec where 120 μmol/m^2/s were used for a photoperiod of 16 hours, this contribution was found to represent 25% (Dorais, 2003). Here, loads of the lighting system (obtained from the supplemental lighting schedule simulation) are input to the thermal model. Changing the lighting system can not only lead to a lower energy bill for supplemental lighting, but also help reducing cooling requirements in the SC farms, where cooling loads represent 30% (in Paris) up to 55% (in Singapore) of total energy loads (see **Figure 6).**

Global Warming Potential (GWP)

In order to compare environmental impacts caused by different resources used by the farms across the four case studies, GHG emissions related to water, energy and transportation were calculated for each scenario and assessed against emissions calculated for the baseline models. Results show that RG farms can considerably reduce GWP in all the cities, in comparison with current supply systems (see **Figure 7**).

The largest share of GHG emissions in the urban BIA farms are related to their high levels of electricity consumption. Their environmental footprint could therefore be further mitigated by associating clean renewable energy sources, such as solar photovoltaic panels, to these systems.

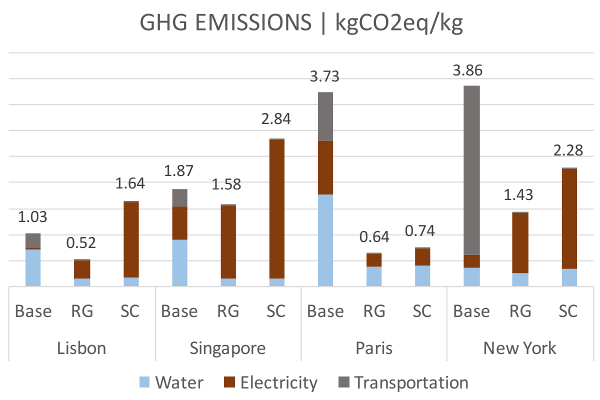

Figure 7: GHG emissions of existing supply systems vs. simulated urban farms.

Table 3 shows GHG emissions caused by the eight simulated BIA farms in comparison with current supply chains for tomato. While RG farms have the potential to reduce GHG emissions under all the tested climates, simulations showed that SC farms are not a desirable solution under mild or hot climates such as in Lisbon or Singapore, not only because of their supplemental lighting requirements, but also because of significant cooling loads (see **Figures 5 and 6**).

Table 3: GHG emissions of simulated models compared to baseline scenarios.

	RG farm	SC farm
Lisbon	50%	159%
Singapore	84%	152%
Paris	17%	20%
New York	37%	59%

The goal of this work was to apply a previously introduced simulation framework for the evaluation of the environmental performance of different BIA typologies, based on climate, crop and geometry of the farm. The above results hence provide a first insight into the type of urban farm solution that should be further assessed in a specific urban area.

The case-studies that were assessed here show that under colder climates such as in Paris or New York, SC farms can reduce GHG emissions by up to 41% in comparison with current supply systems. Such farms can therefore constitute a sustainable solution in these contexts and should be further assessed for energy efficiency optimization, e.g., by improving the insulation layer of the container and/or by testing other lighting solutions. An additional benefit of the shipping container is its portability. Further simulations can therefore model SC farms located indoors, e.g., in warehouses or basements.

Conclusions

This article presented the application of a performance-based workflow model for simulation of Building-Integrated Agriculture (BIA) in early-stage architectural and/or urban design to eight potential urban farms for tomato production located in the four metropolitan areas of Lisbon, Singapore, Paris and New York. The workflow is physics-based and uses reliable inputs from existing literature. It was shown that it provides actionable information for early-stage holistic assessment: whereas Rooftop Greenhouse (RG) farms can significantly reduce GHG emissions under all the tested climates, Shipping Container (SC) farms may only have a positive overall environmental impact in megacities located in colder climates, that seasonally rely on long distance food imports. Going forward this analysis can be adapted to a larger set of crops.

This framework is easy to use by architects and urban planners that work with CAD and BPS tools, and constitutes a first step towards the economic assessment of BIA projects' viability. As the next step of a more comprehensive analysis of a project, a life cycle approach should be considered by the user, in terms of environmental impacts, where the construction and dismantlement phases of the urban farm would be integrated. This full Life Cycle Assessment (LCA) of different BIA typologies should furthermore consider scenarios where operational energy of the farms is provided by in-situ renewable energy sources, such as integrated solar photovoltaic panels, and take account of land use as an additional positive environmental impact related to the implementation of BIA in urban contexts, where no land needs to be converted into cropland. In terms of economic assessment, impacts on local economy should be further assessed, such as business opportunities and jobs created in urbanizing contexts where rural jobs are becoming less attractive.

Acknowledgment

Generous support for this work has been provided by FCT (Portuguese Science and Technology Foundation), under the program MIT Portugal – Sustainable Energy Systems, through the doctoral degree grant SFRH/BD/52306/2013.

References

Albright, L.D., Villiers, D.S. De, 2008. Energy investments and CO2 emissions for fresh produce imported into New York State compared to the same crops grown locally.

Alvarez- Sánchez, E., Leyva-Retureta, G., Portilla-Flores, E., López-Velázquez, A., 2014. Evaluation of thermal behavior for an asymmetric greenhouse by means of dynamic simulations. Dyna 81, 152–159. doi:10.15446/dyna.v81n188.41338

ASHRAE, 2015. ANSI/ASHRAE/IES 2015 Addenda Supplement to ANSI/ASHRAE/IES Standard 90.1-2013, Energy Standard for Buildings Except Low-Rise Residential Buildings.

Barbosa, G., Gadelha, F., Kublik, N., Proctor, A., Reichelm, L., Weissinger, E., Wohlleb, G., Halden, R., 2015. Comparison of Land, Water, and Energy Requirements of Lettuce Grown Using Hydroponic vs. Conventional Agricultural Methods. Int. J. Environ. Res. Public Health 12, 6879–6891. doi:10.3390/ijerph120606879

Benis, K., Ferrao, P., 2016. Potential mitigation of the environmental impacts of food systems through Urban and Peri-Urban Agriculture (UPA) – A Life Cycle Assessment approach. J. Clean. Prod. 140, 784–795. doi:10.1016/j.jclepro.2016.05.176

Benis, K., Reinhart, C., Ferrao, P., 2017. Development of a simulation-based decision support workflow for the implementation of Building-Integrated Agriculture (BIA) in urban contexts. J. Clean. Prod. 147, 589–602. doi:10.1016/j.jclepro.2017.01.130

Carlini, M., Castellucci, S., 2010. Modelling and simulation for energy production parametric dependence in greenhouses. Math. Probl. Eng. 2010. doi:10.1155/2010/590943

De Zwart, H.F., 1996. Analyzing energy-saving options in greenhouse cultivation using a simulation model. PhD Thesis. Landbouwuniversiteit Wageningen.

Despommier, D., 2013. Farming up the city: The rise of urban vertical farms. Trends Biotechnol. 31, 388–389. doi:10.1016/j.tibtech.2013.03.008

Dorais, M., 2003. The use of supplemental lighting for vegetable crop production: light intensity, crop response, nutrition, crop management, cultural practices, in: Canadian Greenhouse Conference. doi:10.1017/CBO9781107415324.004

EnergyPlus, 2016. EnergyPlus weather data [WWW Document]. URL https://energyplus.net/weather

FAO, 2011. Global food losses and food waste - Extent, causes and prevention. Rome.

FAOSTAT, 2013. Food and Agriculture Organization of the United Nations, Statistics Division [WWW Document]. URL http://faostat3.fao.org/home/E

Goldstein, B., Hauschild, M., Fernández, J., Birkved, M., 2016. Testing the environmental performance of urban agriculture as a food supply in northern climates. J. Clean. Prod. 135, 984–994. doi:10.1016/j.jclepro.2016.07.004

Jakubiec, J.A., Reinhart, C.F., 2011. DIVA 2.0: Integrating daylight and thermal simulations using rhinoceros 3D, DAYSIM and EnergyPlus. Proc. Build. Simul. 2011 12th Conf. Int. Build. Perform. Simul. Assoc. 2202–2209.

Kittas, C., Katsoulas, N., Bartzanas, T., Bakker, S., 2013. Greenhouse climate control and energy use, in: FAO (Ed.), Good Agricultural Practices for Greenhouse Vegetable Crops: Principles for Mediterranean Climate Areas. Rome, pp. 63–95.

Kulak, M., Graves, A., Chatterton, J., 2013. Reducing greenhouse gas emissions with urban agriculture: A Life Cycle Assessment perspective. Landsc. Urban Plan. 111, 68–78. doi:10.1016/j.landurbplan.2012.11.007

Lee, C., Costola, D., Loonen, R.C., Hensen, J.L., 2013. Energy saving potential of long-term climate adaptive greenhouse shells, in: Proceedings of Building Simulation 2013: 13th Conference of International Building Performance Simulation Association. pp. 954–961.

Lee, C.S., Costola, D., Swinkels, G.L. a M., Hensen, J.L.M., 2012. On the Use of Building Energy Simulation Programs in the Performance Assessment of Agricultural Greenhouses 1–8.

Marucci, A., Carlini, M., Castellucci, S., Cappuccini, A., 2013. Energy efficiency of a greenhouse for the conservation of forestry biodiversity. Math. Probl. Eng. 2013. doi:10.1155/2013/768658

Mashonjowa, E., Ronsse, F., Milford, J.R., Pieters, J.G., 2013. Modelling the thermal performance of a naturally ventilated greenhouse in Zimbabwe using a dynamic greenhouse climate model. Sol. Energy 91, 381–393. doi:10.1016/j.solener.2012.09.010

McNeel, 2016. Rhinoceros 5.0 [WWW Document]. URL https://www.rhino3d.com/

Pamungkas, A.P., Hatou, K., Morimoto, T., 2014. Evapotranspiration Model Analysis of Crop Water Use in Plant Factory System. Environ. Control Biol. 52, 183–188. doi:10.2525/ecb.52.183

Payen, S., Basset-Mens, C., Perret, S., 2015. LCA of local and imported tomato: An energy and water trade-off. J. Clean. Prod. 87, 139–148. doi:10.1016/j.jclepro.2014.10.007

Puri, V., Caplow, T., 2009. How to grow food in the 100% renewable city: Building-Integrated Agriculture, in: 100% Renewable - Energy Autonomy in Action. London, pp. 229–241.

Reinhart, C.F., Walkenhorst, O., 2001. Validation of dynamic RADIANCE-based daylight simulations for a test office with external blinds. Energy Build. 33, 683–697. doi:10.1016/S0378-7788(01)00058-5

Sanye-Mengual, E., Oliver-Sola, J., Montero, J.I., Rieradevall, J., 2015. An environmental and economic life cycle assessment of rooftop greenhouse (RTG) implementation in Barcelona, Spain. Assessing new forms of urban agriculture from the greenhouse structure to the final product level. Int. J. Life Cycle Assess. 20, 350–366. doi:10.1007/s11367-014-0836-9

Specht, K., Siebert, R., Hartmann, I., Freisinger, U.B., Sawicka, M., Werner, A., Thomaier, S., Henckel, D., Walk, H., Dierich, A., 2014. Urban agriculture of the future: An overview of sustainability aspects of food production in and on buildings. Agric. Human Values 31, 33–51. doi:10.1007/s10460-

013-9448-4

Steel, C., 2008. Hungry city: How food shapes our lives, Random Hou. ed. London.

U.S. Department of Energy, 2016. EnergyPlus 8.6.0 [WWW Document]. URL https://energyplus.net/

United Nations, 2014. World Urbanization Prospects: The 2014 Revision, Highlights (ST/ESA/SER.A/352). doi:10.4054/DemRes.2005.12.9

Vanthoor, B.H.E., 2011. A model based greenhouse design method. Wageningen University.

Villarreal-Guerrero, F., Kacira, M., Fitz-Rodriguez, E., Kubota, C., Giacomelli, G.A., Linker, R., Arbel, A., 2012. Comparison of three evapotranspiration models for a greenhouse cooling strategy with natural ventilation and variable high pressure fogging. Sci. Hortic. (Amsterdam). 134, 210–221. doi:10.1016/j.scienta.2011.10.016

Ward, R., Choudhary, R., Cundy, C., Johnson, G., McRobie, A., 2015. Simulation of plants in buildings, incorporating plant-air interactions in building simulation. Build. Simul. Conf. 2256–2263.

Ward, R.M., Choudhary, R., 2014. A bottom-up energy analysis across a diverse urban building portfolio: retrofits for the buildings at the Royal Botanic Gardens, Kew, UK. Build. Environ. 74, 132–148. doi:10.1016/j.buildenv.2013.12.018

Weber, C.L., Matthews, H.S., 2008. Food-miles and the relative climate impacts of food choices in the United States. Environ. Sci. Technol. 42, 3508–3513. doi:10.1021/es702969f